Microchim Acta (2016) 183:1563–1570
DOI 10.1007/s00604-016-1774-y

ORIGINAL PAPER

Ultrasensitive aptamer-based thrombin assay based on metal enhanced fluorescence resonance energy transfer

Ning Sui[1] · Lina Wang[3] · Fengxia Xie[1] · Fengya Liu[1] · Hailian Xiao[1] · Manhong Liu[1] · William W. Yu[1,2]

Received: 31 October 2015 / Accepted: 1 February 2016 / Published online: 25 February 2016

Abstract A sensitive "on-off" fluorescent protocol for thrombin detection is demonstrated. Firstly, thrombin aptamers which hybridize with labeled help DNA were immobilized on the surface of $Ag@SiO_2$ nanoparticles (NPs). The silver core causes the label Cy5 to display strong metal-enhanced fluorescence. On addition of thrombin and graphene oxide (GO), thrombin (with its high affinity for the aptamers) displaces the Cy5-labeled help DNA which then binds to the surface of GO via π-stacking, causing fluorescence quenching of Cy5. The findings were used to design a thrombin assay that has a 0.05 nM detection limit and excellent selectivity. It was applied to the quantification of thrombin in spiked serum samples where is showed recoveries ranging from 97 % to 107 %, with relative standard deviations between 2.2 and 4.5 %.

Keywords FRET · $Ag@SiO_2$ · Transmission electron microscopy · Graphene oxide · Bioconjugation · Help DNA

✉ Lina Wang
lnwang2006@163.com

✉ William W. Yu
wyu6000@gmail.com

[1] College of Materials Science and Engineering, Qingdao University of Science and Technology, Qingdao 266042, China

[2] Department of Chemistry and Physics, Louisiana State University, Shreveport, LA 71115, USA

[3] College of Environment and Safety Engineering, Key Laboratory of Eco-chemical Engineering, Ministry of Education, Qingdao University of Science and Technology, Qingdao 266042, China

Introduction

Fluorescence detection is one of the most powerful tools in medical diagnostics and biotechnology. [1–3] Much effort has been made to develop fluorescent protocol because of their simplicity, ease of use, and wide-range availability of instrumentation. "Turn-off" and "turn-on" fluorescence responses are the two common processes involved in fluorescent protocol, due to fluorescence quenching or enhancement, respectively. A variety of techniques have been used to manipulate these processes to design platforms for sensing, among which fluorescence resonance energy transfer (FRET) and metal enhanced fluorescence (MEF) are the widely reported techniques. [4–10] FRET assays can adopt a variety of donors (organic dyes, inorganic materials, and metal complexes) and quenchers (organic molecules, metal NPs, and carbon-based nanomaterial quenchers), the sensing is based on the rate of energy transfer from donor to quencher. Donors with high quantum yield (QY) are preferred to obtain high sensitivity, however, some common commercial donors process low quantum yield, such as Cy3 (QY is 0.04), [11] Cy5 (QY is 0.27), [11] NBD (QY is 0.1), [12] which limits the sensitivity of FRET technique. Moreover, photobleaching of organic dyes and photoblinking of quantum dots also limit their applications. MEF can improve the problems above mentioned, to enhance QY, improve photostability, and reduce blinking, endowing this technique high sensitivity. [13–16]

The detection of thrombin with high sensitivity is of great importance in clinical applications, various methods have been developed for thrombin detection. [17–21] Special attentions have been paid on signal amplification strategies, such as rolling circle amplification, [22] nicking enzyme-assisted fluorescent enhancement, [23] and polymerase chain reaction, [24] they have significantly improved the sensitivity for thrombin detection. However, protein enzymes are always

involved in reaction, which are costly and require special reaction conditions. Therefore, development of a simple and sensitive fluorescent method will benefit for thrombin and other targets detection.

Here, we designed an aptamer-based assay for thrombin detection, in which FRET and MEF were both used. A sandwich architecture of Ag@SiO_2-DNA-Cy5 was firstly fabricated. Silver plays the role to enhance fluorescence due to its high efficient MEF effect on Cy5 emission. [15] MEF is dependent upon the distance between the fluorophore and the metal surface, it occurs whenever the distance is from 5 nm to dozens of nanometers. [1, 14, 15] Silica shell was coated on AgNPs to control the distance between metal and fluorophore. GO was chosen as quencher due to its good water dispersity and high-efficiency quenching of fluorescence of dyes. [24, 25] Based on molecular recognition, the fluorescence of Cy5 was enhanced by Ag@SiO_2, and quenched by GO to achieve the purpose of thrombin detection.

Materials and methods

Materials

Tetraethyl orthosilicate (TEOS), N-succinimidyl 4-(N-maleimidomethyl)-cyclohexane-1-carboxylate (sulfo-SMCC), and 3-aminopropyltrimethoxysilane (APTMS) were purchased from Sigma-Aldrich (www.sigmaaldrich.com). All chemicals used in this work were of analytical grade or of highest purity available and used directly without further purification. Milli-Q water (18.2 MΩ•cm) was used in all the preparations. All of the oligonucleotides were synthesized by SBS Genetech Co., Ltd. (Shanghai, China, www.sbsbio.com). Thrombin, bovine serum albumin (BSA), and human IgG antibody were from Zhongshan Golden Bridge Biotechnology Co., Ltd. (Beijing, China, www.zsbio.com). Graphene oxide was purchased from Leadernano Co., Ltd. (Jining, China, www.leadernano.com).

Preparation of Ag and Ag@SiO_2 core/shell NPs

AgNPs were prepared using a previously reported method. [26] Silica coating onto silver NPs was performed by our previous method, [27] Typically, 5 mL of silver colloid was mixed with 20 mL of ethanol (containing 1.25 mL of concentrated ammonia solution) under vigorous stirring. Then, 0.4, 0.7, 1.5, 2.5 and 4 μL of TEOS were added dropwise to the suspension to obtain Ag@SiO_2 NPs with 3, 5, 11, 18, and 26 nm silica shell thickness, respectively. After reacted for 12 h, Ag@SiO_2 NPs were collected by centrifugation and dispersed in 5 mL of ethanol.

Preparation of DNA-functionalized Ag@SiO_2 NPs

The sequences of oligonucleotides (ssDNA) used in this work were as follows: Thrombin aptamer: 5′-SH-$(CH_2)_6$-TACGGTTGGTGTGGTTGG-3′. Help DNA: 5′-Cy5-ACCCAACCACACCAACC-3′

APTMS was used for the functionalization of Ag@SiO_2 NPs with amino groups, which was reported in our previous work. [28] Sulfhydryl-tagged aptamer was covalently conjugated to Ag@SiO_2-NH_2 using sulfo-SMCC as the cross-linking agent. Briefly, 0.2 mg of sulfo-SMCC was added into 5 mL PBS buffer solution (10 mM, containing 20 mM KCl and 2.5 mM $MgCl_2$, pH 6.2) containing 2 mg of Ag@SiO_2-NH_2. After 1 h of reaction, maleimide-activated Ag@SiO_2 NPs were collected by centrifugation, and dispersed in 2 mL HEPES buffer solution, then 5.5 nM (50 μL) of aptamer was added into this solution and reacted overnight at room temperature. Ag@SiO_2-aptamer NPs were collected by centrifugation and incubated in BSA solution (containing 50 nM BSA) to block non-specific adsorption, and washed by HEPES for 3 times. Before thrombin detection, Cy5-labeled help DNA was hybridized with Ag@SiO_2-aptamer to form Ag@SiO_2-aptamer/help DNA, hybridization was performed as below: Ag@SiO_2-aptamer NPs were dispersed in 2 mL hybridization buffer (50 mM Tris-HCl, 1 M NaCl, 0.1 % Tween-20, pH 8.4), 50 μL Cy5-labeled help DNA (containing 10 nM help DNA in 0.05 M borate buffer, pH 8.4) was added in above-mentioned solution, the mixture was incubated at room temperature for 2 h. Finally, the NPs were washed with

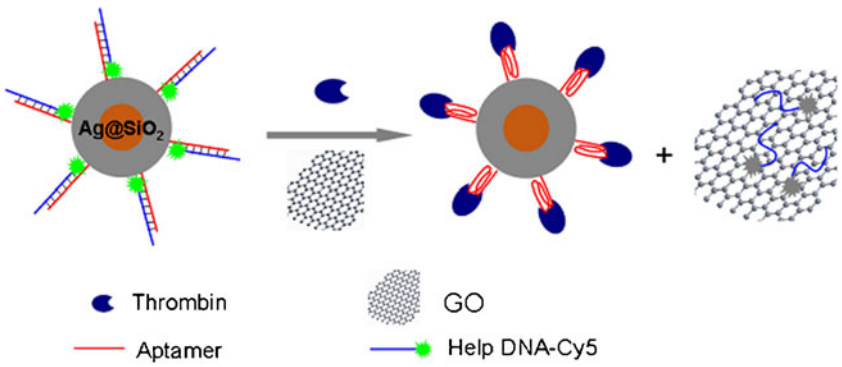

Fig. 1 Schematic illustration of MEF/FRET protocol for thrombin detection

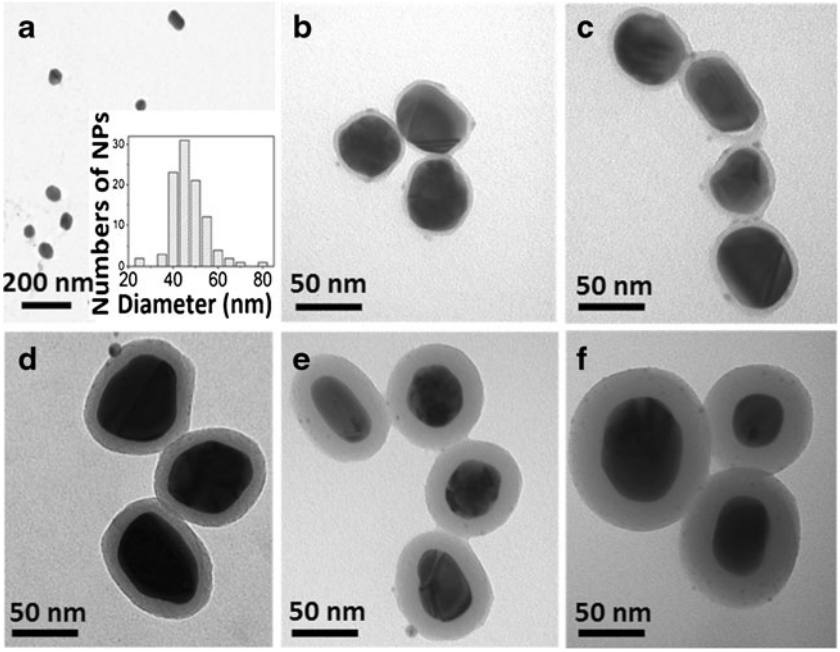

Fig. 2 TEM images of the AgNPs (**a**), and core-shell $Ag@SiO_2$ NPs with 3 ± 1 nm (**b**), 5 ± 1 nm (**c**), 11 ± 1 nm (**d**), 18 ± 1 nm (**e**) and 26 ± 2 nm (**f**) shell thickness

hybridization solution for several times and dispersed in 2 mL hybridization solution for further use.

Thrombin detection

Various concentrations of thrombin were added into $Ag@SiO_2$-aptamer/help DNA (containing 5.5 nM of aptamer and help DNA on surface of $Ag@SiO_2$) and GO (0.3 $mg{\cdot}L^{-1}$) mixture solution, and incubated for 30 min. The selectivity was tested using 10 nM BSA and IgG. For the detection in the serum matrix, freshly serum from a healthy man (Qingdao Central Hospital). Serum is what remains from whole blood after coagulation. Its chemical composition is similar to plasma, but it does not contain coagulation proteins such as thrombin or other factors. All measurements were done in Tris-HCl buffer (20 mM, containing 100 mM NaCl, 5 mM KCl, 1 mM $CaCl_2$, 1 mM $MgCl_2$, and 8.5 % glycerol (*v*/v), pH 7.4). The fluorescence intensities were recorded at 667 nm under 640 nm excitation.

Characterization

JEOL JEM-2010 transmission electron microscope was employed to observe the morphology of $Ag@SiO_2$. The fluorescence emission spectra were measured using a HITACHI F-7000 fluorescence spectrophotometer with an excitation wavelength of 640 nm. The pH was measured on a Lei Ci PHS-3C pH-meter (Shanghai, China).

Results and discussion

The principle of the protocol

The principle of the protocol is illustrated in Fig. 1. The aptamer hybridizes with Cy-5-labeled helper DNA to form rigid DNA duplexes on the surface of the $Ag@SiO_2$ NPs. The fluorescence of Cy5 will be enhanced by silver surface plasmon resonance

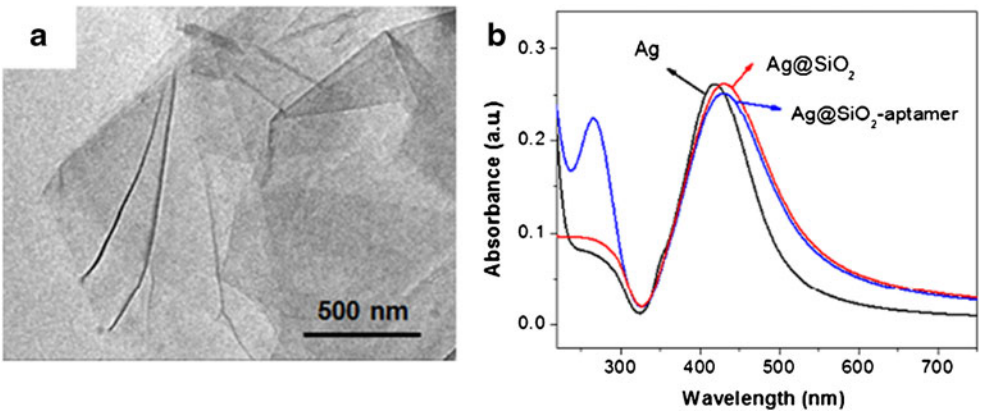

Fig. 3 **a** TEM image of GO, **b** UV-vis absorption spectra of Ag, $Ag@SiO_2$, and $Ag@SiO_2$-aptamer

via controlling the distance between the fluorophore and AgNPs surface (i.e. the thickness of silica shell). Upon the introduction of thrombin and GO, the quadruplex-thrombin complex is formed, [23] the DNA duplexes are dismissed and helper DNA is released which then is absorbed by GO via π-stacking, [29] leading to fluorescence quenching.

Characterization of GO, Ag, and Ag@SiO_2-DNA

The morphology of Ag and Ag@SiO_2 NPs was observed under TEM. The AgNPs with an average diameter of about 49 ± 8 nm (standard deviation for n = 100) were obtained, as shown in Fig. 2a. To achieve MEF effect, silica layer was established between silver and fluorophore to avoid FRET that occurs when the distance between them is below 5 nm, [13, 30] moreover, silica is an optically transparent dielectric medium and plasmon scattering can be achieved up to a few hundreds of nanometers. [31, 32] Herein, various silica thicknesses were fabricated via changing the amount of TEOS, as shown in Fig. 2b-f. The crumpled silk wave-like GO is shown in Fig. 3a. Figure 3b shows the UV-vis absorption of AgNPs, Ag@SiO_2 NPs (11 nm of silica thickness) without and with the functionalization of DNA aptamers. Compared with AgNPs, the peak of Ag@SiO_2 NPs showed a red shift (from 415 to 430 nm) due to the increase of the local refractive index of silica shell. The presence of silica shell facilitates the conjugation of DNA, according to our previous method, [27] the relative ratio of DNA to Ag@SiO_2 was calculated to be about 800 DNA molecules per Ag@SiO_2 nanoparticle. The absorbance at 260 nm proved the successful conjugation of DNA on the surface of Ag@SiO_2 NPs.

MEF between Ag@SiO_2 and Cy5

After hybridization of aptamer and helper DNA, Cy5 can be brought to the surface of Ag@SiO_2, fluorescence enhancement is achieved. The fluorescence intensity of help DNA

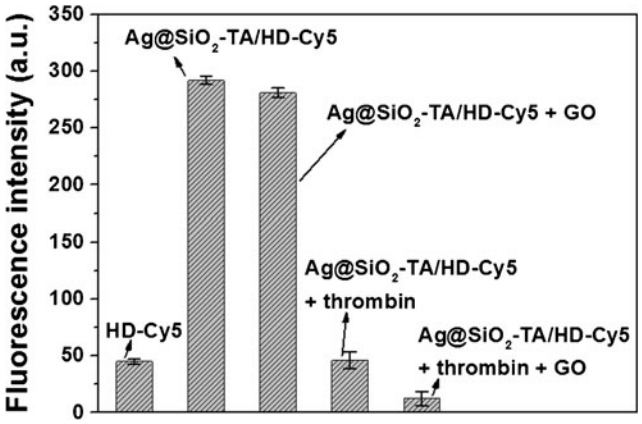

Fig. 5 Fluorescence intensity of HD-Cy5, Ag@SiO_2-TA/HD -Cy5, Ag@SiO_2-TA/HD-Cy5 + GO, Ag@SiO_2-TA/HD-Cy5 + thrombin, Ag@SiO_2-TA/HD-Cy5 + thrombin + GO at 667 nm. HD represents help DNA, TA/HD represents aptamer/help DNA

was monitored before and after the addition of Ag@SiO_2-TA solution, as shown in Fig. 4a. It can be seen that the fluorescence intensity does not increase any more after 10 min, it indicates the DNA hybridization between help DNA and aptamer was accomplished within 10 min. The maximum enhancement factor was 6.3. In the presence of thrombin and GO, the fluorescence intensity decreased gradually, and did not decrease anymore after 20 min, as shown in Fig. 4b. This indicates the formation of quadruplex-thrombin complex and most of the released help DNA was absorbed on GO surface, consequently, FRET occurred between Cy5 and GO due to π-stacking. [29, 33] However, in the presence of only GO, the fluoresence intensity did not change significantly, as shown in Fig. 5. It indicates that the GO can only quench the fluorescence of released help DNA-Cy5.

As MEF is affected by the spatial distance between metal NPs and fluorophore, [10, 13, 26] the distance should be precisely tailored to optimize MEF effect. Here, silica shell was used as separated media, different silica thicknesses

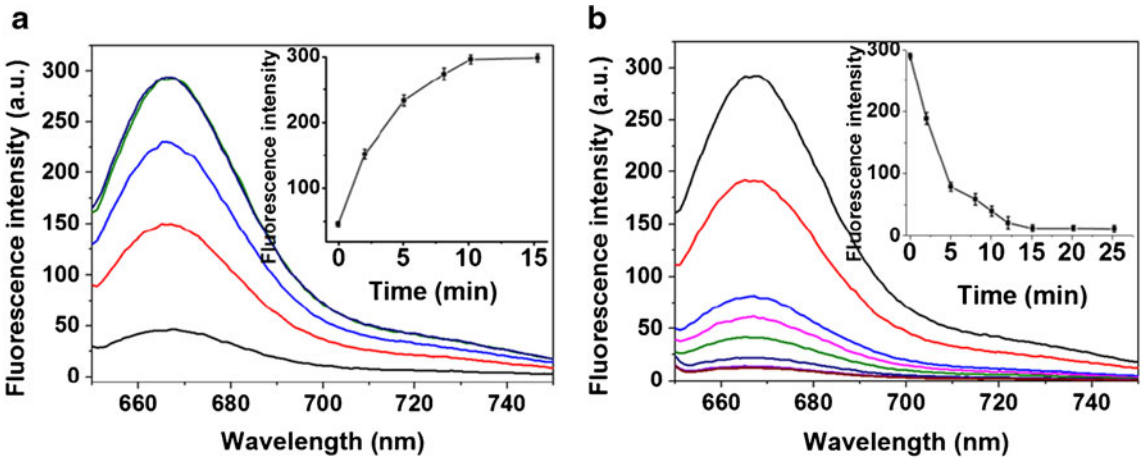

Fig. 4 Fluorescence emission spectra of MEF system (**a**), and MEF/FRET system at 10 nM thrombin concentration (**b**). Insets: fluorescence intensities at 667 nm against the time

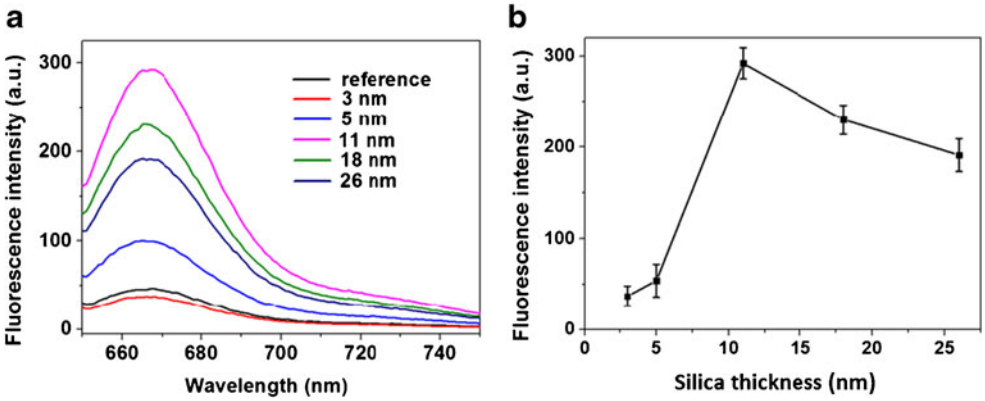

Fig. 6 The fluorescence emission spectra (**a**) and fluorescence intensities at 667 nm (**b**) of different silica thicknesses. Reference is help DNA-Cy5

(3 ± 1 nm, 5 ± 1 nm, 11 ± 1 nm, 18 ± 1 nm, and 26 ± 2 nm, standard deviation comes from ten independent Ag@SiO_2 NPs measurement) were fabricated to evaluate the effect of the separated distance on MEF. At the silica thickness of 3 nm, fluorescence quenching was obtained due to the increased nonradiative decay caused by Ag core, [34] whereas this effect decreased greatly when the separated distance was above 5 nm. Fluorescence enhancement was obtained at other silica thicknesses, and the maximum fluorescence enhancement was achieved when the shell thickness was 11 nm, as shown in Fig. 6. Further increase in silica shell thickness resulted in the decrease of the fluorescence intensity, this is

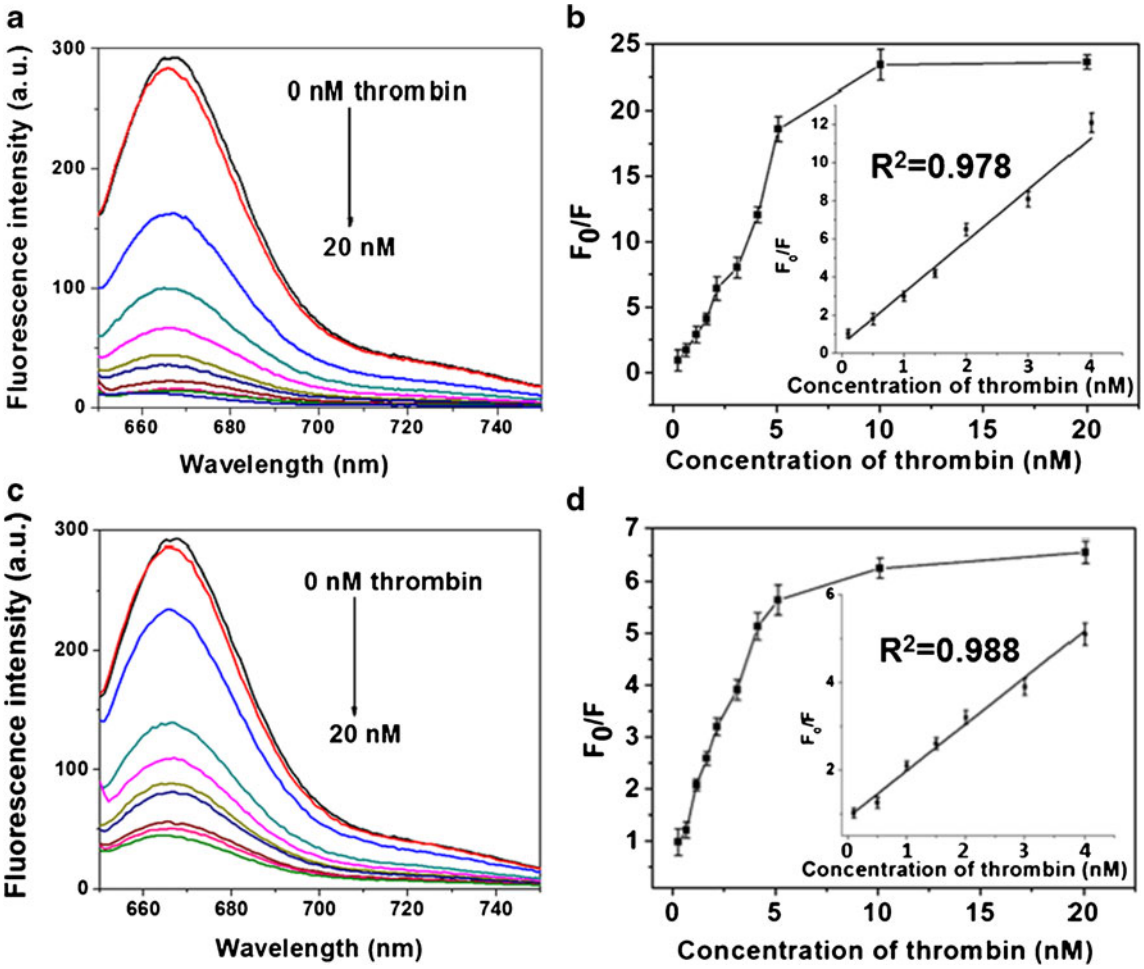

Fig. 7 Fluorescence emission spectra of MEF/FRET assay (**a**) and MEF assay (**c**) in response to different concentrations of thrombin (from top to bottom, 0, 0.1, 0.5, 1.5, 2, 3, 4, 5, 10 and 20 nM). Fluorescence intensity ratio plotted against the concentration of thrombin: MEF/FRET assay (**b**) and MEF assay (**d**). Insets: the linear ranges of sensing assay. F_0 and F were the fluorescence intensity at 667 nm in the absence and presence of thrombin

Table 1 Comparison of fluorescent methods for thrombin detection

Methods	Materials	Analytical ranges (nM)	LOD (nM)	Ref.
FRET	carbon NPs + aptamer	0.5–20	0.18	[36]
FRET	GO + aptamer	–	2	[29]
FRET	magnetic NPs + aptamer	1–60	0.5	[37]
fluorescence	aptamer	0.3–6.5	0.082	[20]
FRET	MnO_2 + aptamer	0–100	11	[38]
MEF/FRET	Ag@SiO_2-aptamer + GO	0.1–4	0.05	this work

because the surface plasmon of Ag did not effectively interact with Cy5. [27, 35]

Thrombin detection

To evaluate the sensitivity of the MEF/FRET protocol, different concentrations of thrombin (0.1, 0.5, 1.5, 2, 3, 4, 5, 10, and 20 nM) and GO were added into the assay, the fluorescence intensity of the assay decreased with the increase of thrombin concentration, as shown in Fig. 7a and b. The plot of the fluorescence intensity ratio F_0/F (F_0 and F were the fluorescence intensity without and with the presence of thrombin and GO) versus the thrombin concentration shows a linear range from 0.1–4 nM with a limit of detection (LOD) 0.05 nM (at a signal-to-noise ratio of 3), we compared our results with other fluorescent methods (Table 1). We also explored another detection approach where the GO was not added into the assay, i.e. only MEF worked. Figure 7c shows the corresponding fluorescence emission spectra, Fig. 7d shows the plot of the fluorescence intensity ratio F_0/F versus the thrombin concentration, the LOD is 0.12 nM. Compared to MEF protocol, MEF/FRET protocol exhibits a higher sensitivity.

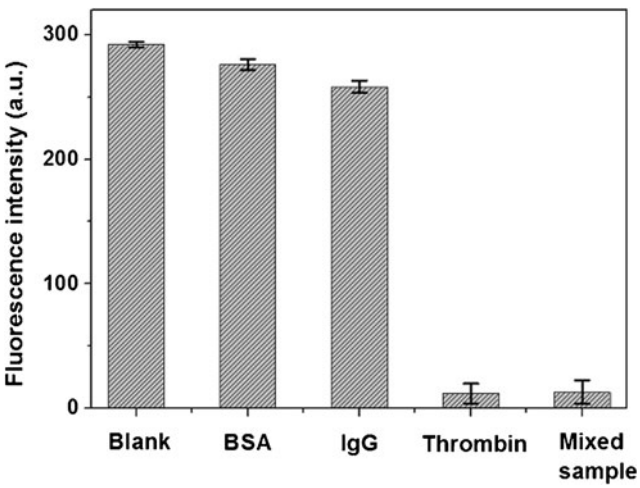

Fig. 8 Selectivity of the MEF/FRET protocol to thrombin (10 nM) by comparing it to the interfering proteins at the same level: BSA, IgG, and the mixed sample (containing 10 nM of thrombin, BSA, and IgG), respectively. Emission wavelength was monitored at 667 nm

Different sensitivity of two detection approaches can be attributed to different fluorescence intensity change in the detection process. After the addition of thrombin, quadruplex-thrombin complex is formed, help DNA is released. The released help DNA exists in solution and is absorbed on GO surface for MEF and MEF/FRET, respectively, leading to different variation of "on-off" fluorescence signals. Obviously, the decrease of fluorescence intensity for MEF/FRET (96 %) is higher than MEF (85 %), thus, the sensitivity of MEF/FRET protocol is higher than MEF protocol.

To check the selectivity of our MEF/FRET protocol, the assay was respectively incubated with 10 nM thrombin, 10 nM BSA, 10 nM human IgG, and a mixture of 10 nM thrombin + 10 nM BSA + 10 nM IgG, the results are shown in Fig. 8. It can be seen that the presence of the BSA and IgG did not show any significant differences compared with the blank, while the incubation of our assay into thrombin, the signal intensity decreased greatly. Similarly, the mixed sample did not exhibit major signal change compared with that of thrombin. The results clearly demonstrated the high specificity of our protocol for thrombin.

Analysis of thrombin in human serum

The MEF/FRET protocol was subsequently applied to monitor the thrombin level in human serum to investigate its practicability. A fresh blood sample from healthy individuals was adopted, the serum samples spiked with different concentrations of thrombin. As presented in Table 2, the recovery for testing of thrombin in the concentration ranged from 97 % - 107 %, and the relative standard deviation ranged from 2.2 % to 4.5 %. It demonstrates the potential of the method for application in complex matrix of serum.

Table 2 Determination of thrombin in human serum

sample	Added (nM)	Found (nM)	RSD (n = 3)	Recovery (%)
1	0.3	0.32	4.5 %	106
2	0.8	0.86	3.1 %	107
3	3.5	3.4	2.2 %	97

Conclusion

We have demonstrated a simple, sensitive, and selective protocol for thrombin detection, which is based on the combination of MEF and FRET fluorescence techniques. The distance of Ag nanoparticle to fluorophore was precisely controlled via tailoring the thickness of silica shell, at the distance of 11 nm, maximum fluorescence enhancement factor of 6 was obtained. The highly efficient MEF combined with FRET effect of GO induced high signaling of the "on-off" format, which in turn led to sensitive for thrombin detection. The system showed the limit of detection of the assay is 0.05 nM, and had a good linear relationship with thrombin concentration in the range of 0.1–4 nM, which was better than MEF system and other FRET sensors. The MEF/FRET system has a wide scope in that it may be adapted to assays for other analytes for which appropriate aptamers can be found. However, rare paper reports MEF/FRET system, the limitation of this system has not been investigated sufficiently, future work will include the application of various types of analytes (biomolecules, metal ions, cells and so on) and the interaction between analytes and GO.

Acknowledgments This work was financially supported by the National Natural Science Foundation of China (21301103, 21501106), the 47th Scientific Research Foundation for the returned overseas Chinese scholars, the taishan scholarship, the Shandong Natural Science Foundation (ZR2012FZ007), the Shandong Province High Education Research And Development program (J13LA08).

Compliance with ethical standards The author(s) declare that they have no competing interests

References

1. Lakowicz JR (2006) Principles of Fluorescence Spectroscopy, Springer; 3rd edition, ISBN: 0387312781
2. Resch-Genger U, Grabolle M, Cavaliere-Jaricot S, Nitschke R, Nann T (2008) Quantum dots versus organic dyes as fluorescent labels. Nat Meth 5:763–775
3. Yang YM, Zhao Q, Feng W, Li FY (2012) Luminescent chemodosimeters for bioimaging. Chem Rev 113:192–270
4. Cheng Z, Li G, Liu M (2015) A metal-enhanced fluorescence sensing platform based on new mercapto rhodamine derivatives for reversible Hg^{2+} detection. J Hazard Mater 287:402–411
5. Li M, Wang QY, Shi XD, Hornak LA, Wu NQ (2011) Detection of mercury(II) by Quantum dot/DNA/Gold Nanoparticle Ensemble based nanosensor via nanometal surface energy transfer. Anal Chem 83:7061–7065
6. Liu XQ, Wang F, Aizen R, Yehezkeli O, Willner I (2013) Graphene oxide/nucleic-acid-stabilized Silver Nanoclusters: functional hybrid materials for optical aptamer sensing and multiplexed analysis of pathogenic DNAs. J Am Chem Soc 135:11832–11839
7. Wang YH, Wu ZJ, Liu ZH (2012) Upconversion fluorescence resonance energy transfer biosensor with aromatic polymer nanospheres as the lable-free energy acceptor. Anal Chem 85:258–264
8. Ma K, Lu L, Qi Z, Feng J, Zhuo C, Zhang Y (2015) In situ induced metal-enhanced fluorescence: A new strategy for biosensing the total acetylcholinesterase activity in sub-microliter human whole blood. Biosen & Bioelectr 68:648–653
9. Li H, Chen C-Y, Wei X, Qiang W, Li Z, Cheng Q, et al. (2012) Highly sensitive detection of proteins based on metal-enhanced fluorescence with novel Silver Nanostructures. Anal Chem 84: 8656–8662
10. Lu L, Qian Y, Wang L, Ma K, Zhang Y (2014) Metal-enhanced fluorescence-based Core shell $Ag@SiO_2$ nanoflares for affinity biosensing via Target-induced structure switching of aptamer. ACS Appl Mat Inter 6:1944–1950
11. Mujumdar RB, Ernst LA, Mujumdar SR, Lewis CJ, Waggoner AS (1993) Cyanine dye labeling reagents: sulfoindocyanine succinimidyl esters. Bioconjug Chem 4:105–111
12. Onoda M, Uchiyama S, Santa T, Imai K (2002) The effects of spacer length on the fluorescence Quantum yields of the benzofurazan compounds bearing a donor acceptor system. Luminescence 17:11–14
13. Lakowicz JR (2001) Radiative decay engineering: biophysical and biomedical applications. Anal Biochem 298:1–24
14. Lakowicz JR (2006) Plasmonics in biology and Plasmon-Controlled Fluorescence. Plasmonics 1:5–33
15. Lakowicz JR, Fu Y (2009) Modification of single molecule fluorescence near metallic nanostructures. Laser Photonics Rev 3: 221–232
16. Ji BT, Giovanelli E, Habert B, Spinicelli P, Nasilowski M, Xu XZ, Lequeux N, Hugonin JP, Marquier F, Greffet JJ, Dubertret B (2015) Non-blinking Quantum dot with a plasmonic nanoshell resonator. Nat Nano 10:170–175
17. Zhang HF, Shuang SM, Sun LL, Chen AJ, Qin Y, Dong C (2014) Label-free aptasensor for thrombin using a glassy carbon electrode modified with a graphene-porphyrin composite. Microchim Acta 181:189–196
18. Xu ZC, Huang XY, Dong CQ, Ren JC (2014) Fluorescence correlation spectroscopy of gold nanoparticles, and its application to an aptamer-based homogeneous thrombin assay. Microchim Acta 181: 723–730
19. Zhang LP, Li L (2015) Colorimetric thrombin assay using aptamer-functionalized gold nanoparticles acting as a peroxidase mimetic. Microchim Acta:1–6
20. Li YB, Ling LS (2015) Aptamer-based fluorescent solid-phase thrombin assay using a silver-coated glass substrate and signal amplification by glucose oxidase. Microchim Acta 182:1849–1854
21. Lin ZH, Pan D, Hu TY, Liu ZP, Su XG (2015) A near-infrared fluorescent bioassay for thrombin using aptamer-modified CuInS2 Quantum dots. Microchim Acta 182:1933–1939
22. Lu CH, Li J, Lin MH, Wang YW, Yang HH, Chen X, Chen GN (2010) Amplified aptamer based assay through catalytic recycling of the analyte. Angew Chem 122:8632–8635
23. Xue LY, Zhou XM, Xing D (2012) Sensitive and homogeneous protein detection based on Target-triggered aptamer hairpin switch and nicking enzyme assisted fluorescence signal amplification. Anal Chem 84:3507–3513
24. Pérez-López B, Merkoçi A (2012) Carbon nanotubes and graphene in analytical sciences. Microchim Acta 179:1–16
25. Duan Y, Ning Y, Song Y, Deng L (2014) Fluorescent aptasensor for the determination of salmonella typhimurium based on a graphene oxide platform. Microchim Acta 181:647–653
26. Deng W, Jin DY, Drozdowicz-Tomsia K, Yuan JL, Wu J, Goldys EM (2011) Ultrabright Eu-Doped Plasmonic $Ag@SiO_2$ nanostructures: time-gated bioprobes with single particle sensitivity and negligible background. Adv Mater 23:4649–4654
27. Sui N, Wang LN, Yan TF, Liu FY, Sui J, Jiang YJ, Xiao HL, Liu MH, Yu WW (2014) Selective and sensitive biosensors based on metal-enhanced fluorescence. Sensors and Actuators B: Chem 202: 1148–1153

28. Yang LT, Ellington AD (2008) Real-time PCR detection of protein analytes with conformation-switching aptamers. Anal Biochem 380:164–173
29. Lu CH, Yang HH, Zhu CL, Chen X, Chen GN (2009) A graphene platform for sensing biomolecules. Angew Chem 121:4785–4787
30. Haldar KK, Sen T, Patra A (2010) Metal conjugated semiconductor hybrid nanoparticle-based fluorescence resonance energy transfer. J Phys Chem C 114:4869–4874
31. Sui N, Monnier V, Zakharko Y, Chevolot Y, Alekseev S, Bluet J-M, Lysenko V, Souteyrand E (2012) Fluorescent (Au@SiO_2)SiC nanohybrids: influence of Gold nanoparticle diameter and SiC nanoparticle surface density. Plasmonics 8:85–92
32. Sui N, Monnier V, Zakharko Y, Chevolot Y, Alekseev S, Bluet J-M, Lysenko V, Souteyrand E (2012) Plasmon-controlled narrower and blue-shifted fluorescence emission in (Au@SiO_2)SiC nanohybrids. J Nanoparticle Res 14:1–10
33. Li F, Chao J, Li ZH, Xing S, Su S, Li XX, Song SP, Zuo XL, Fan CH, Liu B, Huang W, Wang LH, Wang LH (2015) Graphene oxide-assisted nucleic acids assays using conjugated polyelectrolytes-based fluorescent signal transduction. Anal Chem 87:3877–3883
34. Bharadwaj P, Novotny L (2007) Spectral dependence of single molecule fluorescence enhancement. Opt Express 15:14266–14274
35. Pang YF, Rong Z, Xiao R, Wang SQ (2015) "Turn on" and label-free core shell Ag@SiO_2 nanoparticles-based metal-enhanced fluorescent (MEF) aptasensor for Hg^{2+}, Sci Rep 5. 9541:1–5
36. Wang Y, Bao L, Liu Z, Pang D-W (2011) Aptamer biosensor based on fluorescence resonance energy transfer from upconverting phosphors to carbon nanoparticles for thrombin detection in human plasma. Anal Chem 83:8130–8137
37. Yu JM, Yang LR, Liang XF, Dong TT, Liu HZ (2015) Bare magnetic nanoparticles as fluorescence quenchers for detection of thrombin. Analyst 140:4114–4120
38. Wang C, Zhai W, Wang Y, Yu P, Mao L (2015) MnO_2 nanosheets based fluorescent sensing platform with organic dyes as a probe with excellent analytical properties. Analyst 140:4021–4029